



Final Report Zeehan SkyTEM Survey



Geoforce Job Number: SK987MI

Authors: James Reid, Tristan Kemp, Russell Eade

Table of Contents

| | | |
|------------|---|----|
| 1 | Summary | 3 |
| 2 | Personnel | 4 |
| 2.1 | Field Operations | 4 |
| 2.2 | Base Operations | 4 |
| 3 | Flight plan | 5 |
| 4 | Logistics | 6 |
| 5 | Geometry | 6 |
| 5.1 | Sign conventions | 6 |
| 6 | SkyTEM System specifications | 9 |
| 7 | SkyTEM data processing..... | 11 |
| 7.1 | Known data issues | 11 |
| 7.2 | EM Signal Bias Removal | 11 |
| 7.3 | EMaxAir processing..... | 13 |
| 8 | Magnetometers | 14 |
| 9 | Magnetics Processing | 15 |
| 10 | GPS Positioning | 16 |
| 11 | Navigation | 16 |
| 12 | Altimeters | 16 |
| 13 | References | 17 |
| Appendix A | Survey Specifications | 18 |
| Appendix B | Transmitter current waveform measurements | 19 |
| Appendix C | High altitude tests | 24 |
| Appendix D | Header for high moment SkyTEM data | 25 |
| Appendix E | Header for low moment SkyTEM data..... | 28 |
| Appendix F | Header for TMI data | 31 |
| Appendix G | Header for CDI data | 33 |
| Appendix H | Header for conductivity-depth slice data..... | 34 |
| Appendix I | Deliverables on DVD | 36 |

1 Summary

| | |
|-------------------------|---|
| Geoforce Job Number | SK987MI |
| Survey Company | Geoforce Pty Ltd |
| Dates Flown | 20 th January – 30 th January 2009 |
| Client | Zeehan Zinc Ltd. |
| Terrain Clearance | 30 m (nominal) |
| Total Line km | 1572 |
| Datasets acquired: | Time-domain EM Total Magnetic Intensity Digital Terrain Model |
| EM System | SkyTEM (Interleaved Low and High Moment) |
| Helicopter company | HeliWest, Perth, WA |
| Helicopter type | AS350 Super D2 |
| Helicopter registration | VH-NRW |
| Traverse Line Spacing | 100 m |
| Traverse Line Direction | 090 – 270 |
| Tie Line Spacing: | 1000 m |
| Tie Line Direction | 000 - 180 |
| Navigation | DGPS |
| Coordinate System | AMG55 / AGD66 |

2 Personnel

The following personnel were employed for this project:

2.1 Field Operations

| | |
|----------------------|---|
| Crew Chief | Campbell Greenwood |
| Technical Assistants | Chris Ward-Allen, Samantha Long, Brett Rees |
| Pilot | Ian Pullan |

2.2 Base Operations

| | |
|-----------------|-----------------------------|
| Project Manager | James Reid |
| Data Processing | Russell Eade, Tristan Kemp. |

3 Flight plan

The flight plan and line numbers are shown in Figure 3-1.

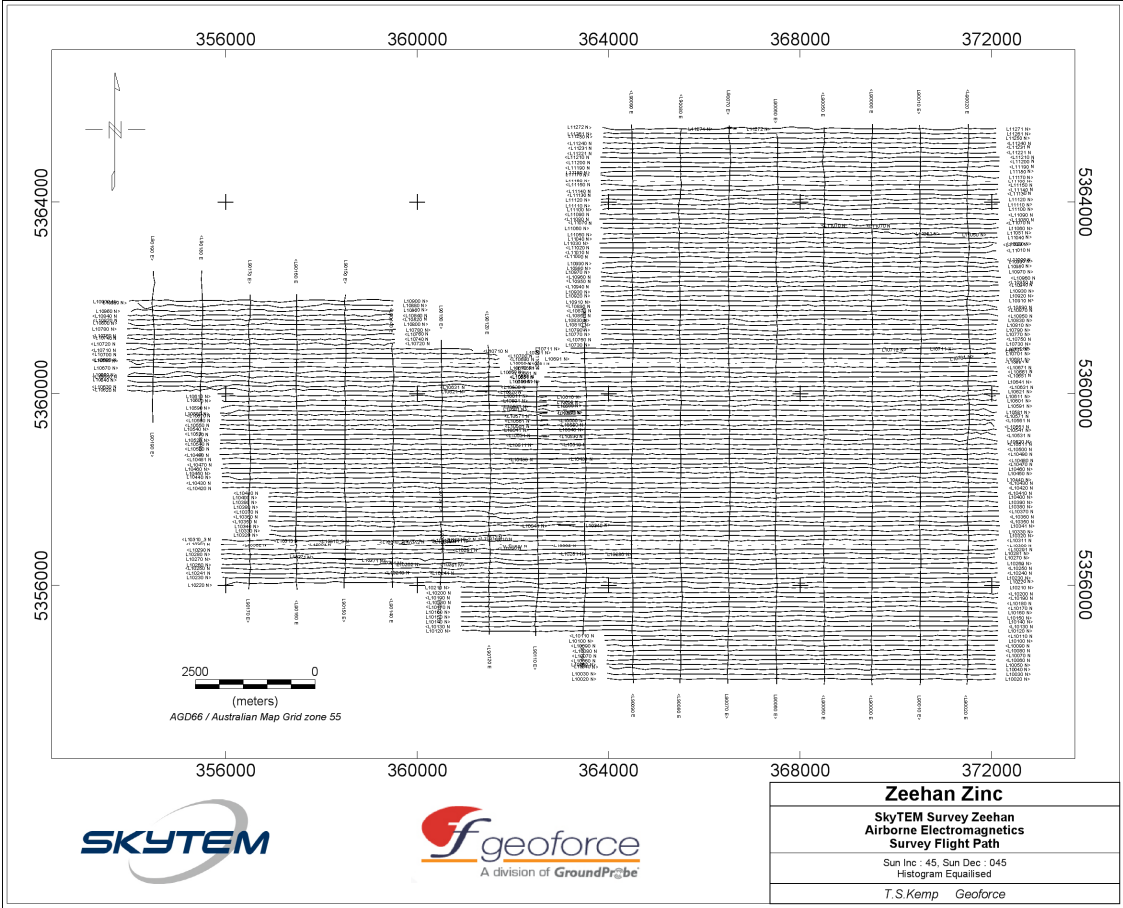


Figure 3-1: Flight path map for Zeehan SkyTEM Survey (AMG55/AGD66 coordinates).

4 Logistics

The survey was flown between 20th January and 30th January, 2009. Rain, high winds and low cloud reduced production rates although the survey was completed without incident in an acceptable timeframe.

A logistics summary report is provided on DVD (SK987MI_logistics Report.pdf).

5 Geometry

Geometry of the system is illustrated below. X, Y and Z coordinates of each sensor are given with respect to the centre of the Tx loop. The Z-coordinate is positive above the Tx loop wire. Positive X and Y-axes are in the flight direction and to the starboard side respectively.

Sensors are as follows:

| | |
|---------------|--|
| Z-coil: | EM Z-axis sensor |
| X-coil: | EM X-axis sensor |
| Tilt1: | Tiltmeter set 1 (measures tilts from horizontal with respect to both X and Y axes) |
| Tilt2: | Tiltmeter set 2 (measures tilts from horizontal with respect to both X and Y axes) |
| Alt1: | Laser Altimeter 1 |
| Alt 2: | Laser Altimeter 2 |
| GP1: | GPS 1 Antenna |
| GP2: | GPS 2 Antenna (RTK DGPS via Fugro Omnistar HP Service) |
| Magnetometer: | G-822A caesium magnetometer sensor |

5.1 Sign conventions

Vertical (Z) -component electromagnetic data measured over a purely-conductive (non-polarizable) one-dimensional earth is positive. Early-time Z-component negatives are sometimes observed in very resistive areas due to the transmitter bias, if it has not been removed from the measured data. Late time Z-component negatives are occasionally observed due to induced polarization effects.

Horizontal inline (X) -component electromagnetic data is positive in the flight direction: The X-component response measured over a purely-conductive (non-polarisable) one-dimensional earth is typically negative. However, X-component data is strongly affected by frame tilt, which can introduce a large contribution from the much-stronger Z-component response

and significantly distort the measured X-component response. The only rigorous way to account for this effect in the data is to explicitly include the transmitter loop tilts in the X and Y directions in the forward/inverse modelling algorithm used to interpret the data.

AngleX (measured by both Tilt1 and Tilt2) **is positive when the nose of the transmitter loop frame is pitched up**, ie over level ground, AngleX is positive when the nose of the frame is further from the ground than the base of the tail rudder.

AngleY (measured by both Tilt1 and Tilt2) **is positive when the starboard side of the transmitter loop frame is tilted down** ie over level ground, AngleY is positive when the starboard side of the frame is closer to the ground than the port side.

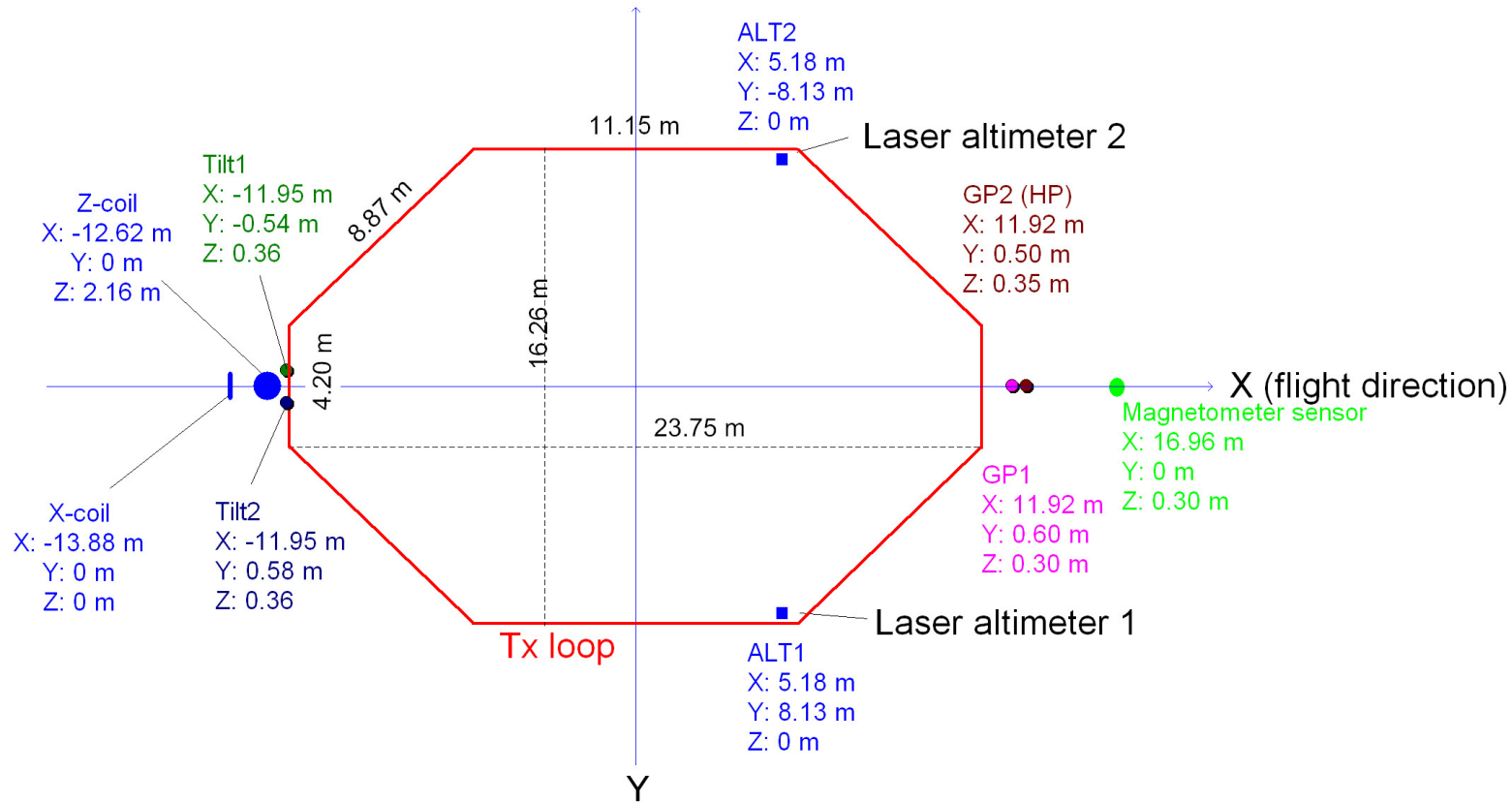


Figure 5-1: Sensor geometry for Zeehan SkyTEM survey. See main text for explanatory notes.

6 SkyTEM System specifications

| | |
|-------------------------------------|----------------------------------|
| EM Transmitter – High Moment | |
| Transmitter loop area | 314 m ² |
| Number of transmitter loop turns | 4 |
| Average peak current | 96.73 A |
| Peak moment | 121,493 A.turn.m ² |
| Tx loop height (nominal) | 30 m |
| Tx Waveform – High Moment | |
| Base frequency | 25 Hz |
| Tx duty cycle | 50% |
| Tx waveform | Bipolar |
| Tx on-time | 10 ms |
| Tx off time | 10 ms |
| Tx ramp time | 44 μs |
| EM Transmitter – Low Moment | |
| Transmitter loop area | 314 m ² |
| Number of transmitter loop turns | 1 |
| Average peak current | 40.63 A |
| Peak moment | 12,758 A.turn.m ² |
| Tx loop height (nominal) | 30 m |
| Tx Waveform – Low Moment | |
| Base frequency | 222.22 Hz |
| Tx duty cycle | 44.4% |
| Tx waveform | Bipolar |
| Tx on-time | 1 ms |
| Tx off time | 1.25 ms |
| Tx ramp time | 10.0 μs |

Table 6-1: Skytem Tx specifications.

| | |
|---|---------------------|
| EM Receiver | |
| EM Sensors | dB/dt coils |
| Rx coil effective area (Z and X) | 31.4 m ² |
| Low pass cut-off frequency for Rx coils | 450 kHz |
| Low pass cut-off frequency for Rx electronics | 300 kHz |
| Z-component Rx coil position | |
| Behind Tx loop centre | 12.62 m |
| Above plane of Tx loop | 2.16 m |
| X-component Rx coil position | |
| Behind Tx loop centre | 13.88 m |
| Above plane of Tx loop | 0 m |

Table 6-2: Skytem Rx specifications.

7 SkyTEM data processing

Raw (binary) SkyTEM data have been processed using the proprietary software package SkyPro (Build 43) to generate ASCII data files. All positions, altitudes etc in processed data are relative to the centre of the transmitter loop. Altitudes have been corrected for Tx loop attitude, and are averages of data from both altimeters following application of a local maximum filter. Electromagnetic data have been stacked using a moving average filter of width 2 seconds, representing a stack of ~80 transients for high moment data and ~160 transients for LM data.

Stacked data have been output every 0.25 seconds (~6 m on the ground at 80km/h groundspeed).

Units for processed data are $V(A.turns.m^4)$, ie voltage normalized by transmitter area \times number of turns \times peak current \times receiver area).

7.1 Known data issues

Due to the steep terrain and high winds, effects from variations in height can be seen in the magnetic dataset. The effects are minor but must be taken into consideration when performing interpretations based on this dataset.

7.2 EM Signal Bias Removal

A design feature of the SkyTEM system is the low transmitter bias signal, which usually means it is not necessary to subtract the bias from the measured data (see document SKYTEM technical overview January August 2008.pdf included on DVD). However, transmitter bias becomes significant in resistive areas, where the early time signal arising from the earth has very low amplitude. Transmitter bias effects were clearly visible in preliminary processed data for the Zeehan survey (see Figure 7-1). Accordingly, the transmitter bias signal was determined from high-altitude data and subtracted from the processed data prior to generation of CDIs. The bias signal at each channel was determined by averaging the biases measured during high-altitude flights conducted at the start and end of the Zeehan survey. Bias signals for each channel are given in Table 7.1. The effect of subtracting the transmitter bias from the raw data is illustrated in Figure 7-1. All EM xyz files and derived data on the DVD have had the bias removed.

| Channel | Gate Centre (microsec) | Mean X LM V/(A.turns.m4) | Mean Z LM V/(A.turns.m4) | Mean X HM V/(A.turns.m4) | Mean Z HM V/(A.turns.m4) |
|---------|---------------------------|-----------------------------|-----------------------------|-----------------------------|-----------------------------|
| 4 | 14.2 | -3.19454E-10 | -7.29514E-11 | | |
| 5 | 18.2 | -2.47053E-10 | 1.73204E-11 | | |
| 6 | 22.7 | -1.16823E-10 | 1.99322E-11 | | |
| 7 | 28.7 | -5.39914E-11 | 1.32127E-11 | | |
| 8 | 36.2 | -2.59867E-11 | 7.54855E-12 | | |
| 9 | 45.2 | -1.36867E-11 | 5.59025E-12 | | |
| 10 | 56.7 | -8.52815E-12 | 3.60087E-12 | -4.69892E-11 | -3.31849E-11 |
| 11 | 71.2 | -6.37839E-12 | 2.10363E-12 | -2.40152E-11 | -1.61374E-11 |
| 12 | 89.7 | -1.38492E-12 | 1.08742E-12 | -1.10195E-11 | -7.29252E-12 |
| 13 | 113.2 | -1.73614E-12 | 5.14495E-13 | -4.24778E-12 | -2.64033E-12 |
| 14 | 142.2 | 2.91447E-13 | 3.31492E-13 | -1.38853E-12 | -6.85274E-13 |
| 15 | 179.2 | -4.2763E-13 | 8.28482E-14 | -3.43171E-13 | -7.33683E-14 |
| 16 | 225.7 | 6.69197E-14 | 1.38172E-14 | -7.37083E-14 | 8.25241E-14 |
| 17 | 283.7 | -9.0643E-14 | 4.67963E-14 | 7.87737E-16 | 9.61346E-14 |
| 18 | 357.2 | -1.77833E-13 | 7.9488E-15 | -2.09716E-14 | 4.74422E-14 |
| 19 | 449.7 | -3.45686E-14 | 6.85559E-14 | -4.74319E-15 | 3.96406E-14 |
| 20 | 566.2 | -8.14138E-14 | 3.75994E-14 | 4.01375E-15 | 1.63915E-14 |
| 21 | 712.7 | -6.18121E-14 | -8.65178E-15 | -5.28815E-15 | 1.16644E-14 |
| 22 | 897.2 | -3.62992E-14 | -1.07022E-14 | 2.00006E-15 | 3.69066E-15 |
| 23 | 1129.7 | | | 1.17953E-14 | 7.29733E-15 |
| 24 | 1422.2 | | | 4.70945E-15 | 1.14718E-14 |
| 25 | 1790.2 | | | 7.23201E-16 | 6.04685E-15 |
| 26 | 2253.7 | | | -3.47943E-16 | 7.13208E-15 |
| 27 | 2837.2 | | | -6.53288E-15 | 2.44317E-15 |
| 28 | 3571.7 | | | -1.25703E-14 | -3.65418E-16 |
| 29 | 4496.7 | | | -1.44031E-14 | 4.75859E-15 |
| 30 | 5661.2 | | | -1.05575E-14 | 5.92297E-15 |
| 31 | 7126.7 | | | 6.36164E-15 | 3.21785E-15 |
| 32 | 8843.2 | | | 1.84276E-14 | 4.84841E-15 |

Table 7-1: Transmitter biases determined by averaging high altitude data recorded at the start and end of the Zeehan survey.

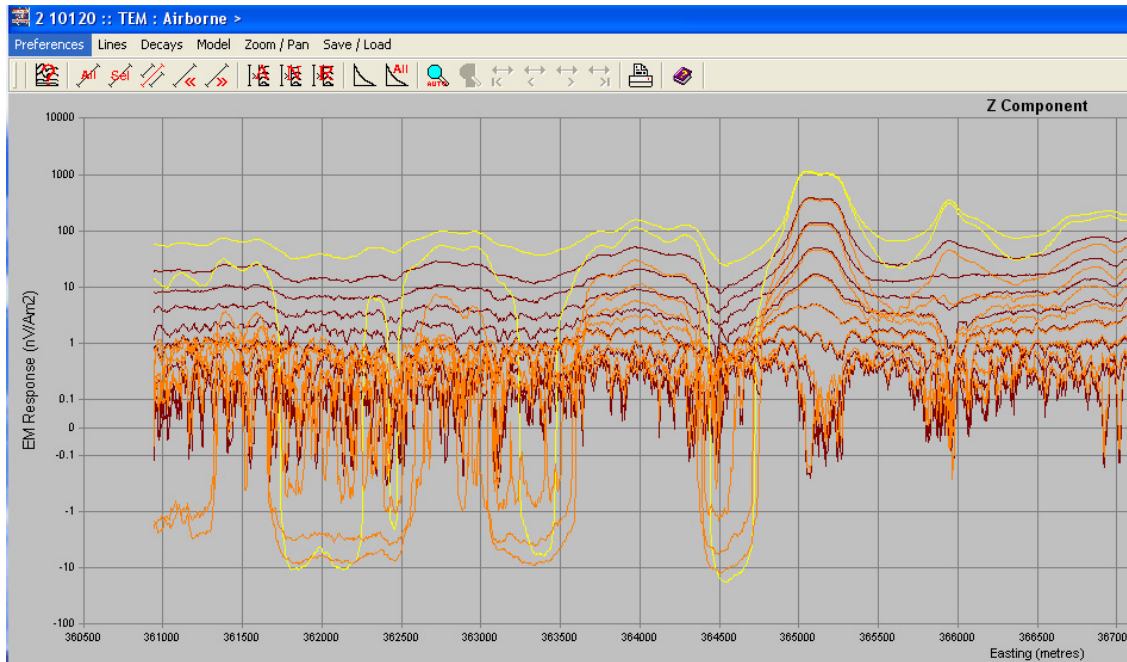


Figure 7-1: Comparison of raw Z channel biased EM signal to raw Z channel EM signal with bias removed displayed in *Maxwell* software. Bias affected EM signal coloured orange, bias removed signal coloured red. Note that the early time response is negative in the bias affected data due to the bias signal being greater than the earth response.

7.3 EMaxAir processing

Z-component XYZ data have been converted to apparent conductivity vs. depth using EMax_air v2.24a (Fullagar and Reid, 2001). The apparent conductivity data have been ‘sharpened’ in order to yield improved depth resolution of conductive layers. The sharpening process treats the apparent conductivity (σ_a) generated by the initial transformation as a depth average, ie

$$\sigma_a(z) = \frac{1}{z - z_0} \int_{z_0}^z \sigma(u) du$$

The above equation can be inverted for the ‘sharpened’ conductivity, which provides improved depth resolution of conductive layers.

$$\sigma(z) = \sigma_a(z) + (z - z_0) \frac{d\sigma_a}{dz}(z)$$

Figure 7-2 compares original and sharpened apparent conductivity curves for a synthetic three-layered model.

Conductivity-depth data files have extension *.CDI. A complete description of the CDI file format can be found in Appendix G.

Images of CDI sections for each flight line are also provided on DVD.

Average conductivities in a number of 'depth slices' below surface have also been computed and are provided both as ASCII data. The ASCII file format for the conductivity depth slices is given in Appendix H.

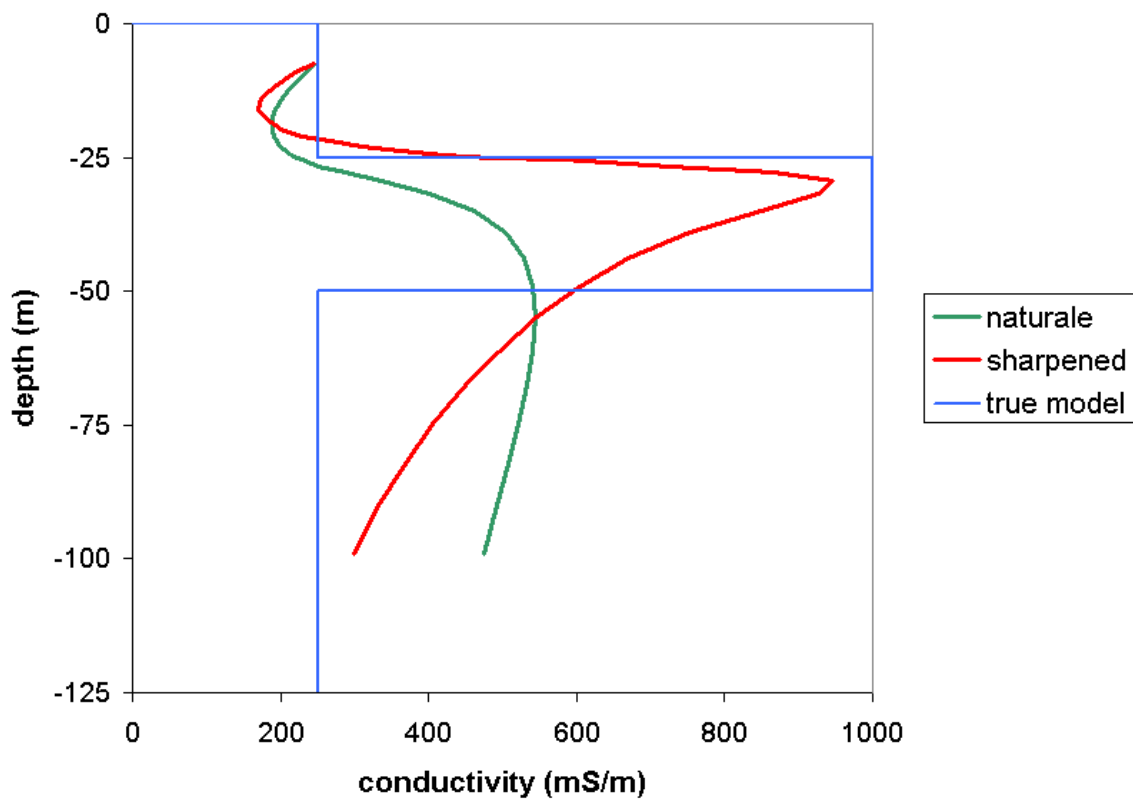


Figure 7-2: Comparison of original (green) and sharpened (red) conductivity-depth curves for a synthetic three-layer model (blue) (Fullagar et al., 2008)

8 Magnetometers

Raw and processed magnetic data are provided with this report. Raw magnetic data is given in the 'raw' column in the located magnetics data. Raw data has undergone pre processing only (spike removal, short gaps interpolated, low pass filtering, but not corrected for heading, diurnal, IGRF, or levelled).

The airborne magnetometer samples only during the off time of the high moment EM measurements – not during either low-moment or noise measurements.

| | |
|----------------------|--|
| Airborne Sensor | Geometrics G-822A Caesium Magnetometer |
| Sample Rate | 0.1 sec / 2 - 4 m |
| Magnetometer Counter | KroumVS Instruments KMAG4 |
| Base Magnetometer: | Geometrics G-856 |
| Sample Rate: | 5 sec |

The base magnetometer was located at: 362,941 E, 5,361,092 N (AMG55/AGD66).

9 Magnetics Processing

Final Easting, Northing (X, Y) positions were derived from RTK DGPS (Fugro Omnistar HP real-time correction).

The diurnal base station data was analyzed for spikes and spurious sections which were manually removed from the dataset. A 10 point low pass filter was then applied to the diurnal data. A base value of 61866.44nT was established by averaging all readings acquired at the base over the survey duration and this value was subtracted from the base values to determine a diurnal correction.

Magnetic survey data was inspected for spikes and spurious segments which were removed manually. Short gaps (less than 50m) were linearly interpolated. Gaps larger than 50m were not interpolated.

The diurnal correction was removed from the magnetic survey data by synchronizing the diurnal data time and the roving magnetics system time. The diurnally corrected magnetics survey data was then low pass filtered using a filter width of 25m.

System lag was analyzed from series of test and survey lines flown in opposite directions. The system lag is negligible at +0.1 sec, nevertheless a lag correction was applied.

Heading error was analyzed from test data. The Skytem system has no compensation system so a heading correction is necessary. A heading correction of ± 7.8 nT was applied for traverse lines and ± 10 nT for tie lines, with the sign of the correction dependent on the flight direction.

The updated IGRF 2005 correction was calculated at each data point and applied to the data.

Tie line leveling was applied to the data by least squares minimization, using a DC shift only option. Micro-leveilling was selectively applied to areas of the data where leveling problems persisted to remove the minor variations in profile intensity. Selective micro-leveilling of the data maintains the integrity of data that does not need harder leveling techniques.

The final data sets consisted of a RMF, (Residual Magnetic Field – filtered, corrected for, lag, heading, diurnal, IGRF, levelled, microlevelled), and a TMI (Total Magnetic Field = RMF + IGRF).

Located and gridded data were generated from the final processed magnetic data.

10 GPS Positioning

Two GPS receivers were employed for the Zeehan survey (see Section 5 above). GP1 is a standard GPS unit for which differentially-corrected positions are obtained via post-processing in conjunction with data from a ground base station recorded at 1 second intervals. GP2 is a real-time kinematic (RTK) unit for which differential corrections are received in real time from the Fugro Omnistar HP service.

All processed data delivered with this report uses elevations and positions from GP2. Elevation data are relative to the GRS80 ellipsoid corrected to AHD in the DTM channel only.

11 Navigation

Navigation was done through the proprietary software SkyMap version 19 using flight lines created by Geoforce and approved for use by Kate Godber of Mitre Geophysics. Accurate frame location was obtained from the RTK Omnistar HP GPS2 unit via a radio modem feed. Height above ground of the frame was obtained from the two laser altimeters mounted on the frame via the radio modem. There was also a backup radar altimeter used in the helicopter. Through SkyMap the pilot could also monitor the frame tilt and groundspeed to ensure the best possible data was obtained.

12 Altimeters

| | |
|----------------------|-------------------|
| Laser Altimeter: | LaserAce IMHR 300 |
| Reflectorless Range: | 2 – 150 m |
| Accuracy: | 0.2 m |
| Resolution: | 0.1 m |

13 References

Fullagar, P.K., and Reid, J.E., 2001, EMax conductivity-depth transformation of airborne TEM data: Expanded Abstracts, Australian Society of Exploration Geophysicists 15th Conference, Brisbane.

Fullagar, P. K., Reid, J. E., and Pears, G., 2008, Advances in EMaxAir conductivity-depth imaging of airborne TEM data: Conference presentation, 5th international conference on airborne electromagnetics, Haikko Manor, Finland, 28-30 May 2008.

Appendix A Survey Specifications

A.1 Groundspeed

The mean survey groundspeed for the survey was 65.1km/h. Average values have been calculated for each line: these range from 38.1km/h to 85km/h.

A.2 Terrain clearance

The mean terrain clearance for the survey was 37.6m. Average altitudes for each survey line ranged from 26.7m to 102m.

A full report of line statistics is included on DVD (SK987MI_Line_Statistics.xlsx).

Appendix B Transmitter current waveform measurements

Transmitter current waveforms were measured on the ground on 20th January 2009.

The current turnon was measured using a Fluke 80i-100s current clamp and PicoScope ADC212 digital oscilloscope.

The turnoff was measured using a custom-built pickup coil (serial number Pickup 01) and a PicoScope ADC212 digital oscilloscope. The pickup coil measures the time rate of change of current.

Current turnon and (dl/dt) turnoff data have been processed using WaveFormInv, an inversion code written by Niels Christensen of the University of Aarhus. WaveFormInv reconstructs the waveform from the I (turnon) and dl/dt (turnoff) measurements, and generates a piecewise linear approximation to the waveform.

The piecewise linear waveforms are given below and are supplied with this report in ASCII format files (*.wfn). The waveforms are normalized by peak current such that a normalized current of 1 corresponds to the peak transmitter current.

The *.wfn files contain two header lines, followed by the waveform data (two columns). The first column of the waveform data is time in seconds (time zero = start of current switch off), and the second column is normalized current.

Figures B1 and B2 show examples of the high and low-moment waveforms measured using the Fluke current clamp.

Figures B3 and B5 show examples of measured turn on waveforms for high and low-moment respectively.

Figures B4 and B6 show examples of measured turn-off ramps for high- and low-moment respectively.

B.1 Piecewise approximation to high moment current waveform

Time zero is the start of current turnoff. Normalised current is actual current normalized by peak current.

20th January 2009

| <i>Time (sec)</i> | <i>Normalised current</i> |
|-------------------|---------------------------|
| -1.000e-002 | 0.000e+000 |
| -8.394e-003 | 4.588e-001 |
| -6.394e-003 | 7.548e-001 |
| -3.799e-003 | 9.217e-001 |
| 0.000e+000 | 1.000e+000 |
| 4.099e-007 | 9.984e-001 |
| 8.055e-007 | 9.917e-001 |
| 1.254e-006 | 9.805e-001 |
| 3.560e-006 | 9.201e-001 |
| 2.109e-005 | 4.600e-001 |
| 3.863e-005 | 1.011e-002 |
| 3.926e-005 | 4.047e-003 |
| 4.005e-005 | 1.096e-003 |
| 4.115e-005 | 1.568e-004 |
| 4.395e-005 | 0.000e+000 |

B.2 Piecewise approximation to low moment current waveform

Time zero is the start of current turnoff. Normalised current is actual current normalized by peak current.

20th January 2009

| <i>Time (sec)</i> | <i>Normalised current</i> |
|-------------------|---------------------------|
| -1.000e-003 | 0.000e+000 |
| -9.199e-004 | 6.371e-001 |
| -7.994e-004 | 9.209e-001 |
| -6.165e-004 | 9.922e-001 |
| 0.000e+000 | 1.000e+000 |
| 4.794e-007 | 9.903e-001 |
| 8.999e-007 | 9.487e-001 |
| 1.386e-006 | 8.683e-001 |
| 2.440e-006 | 6.648e-001 |
| 4.142e-006 | 3.340e-001 |
| 5.844e-006 | 5.867e-002 |
| 6.338e-006 | 2.348e-002 |
| 6.949e-006 | 6.359e-003 |
| 7.806e-006 | 9.099e-004 |
| 9.995e-006 | 0.000e+000 |

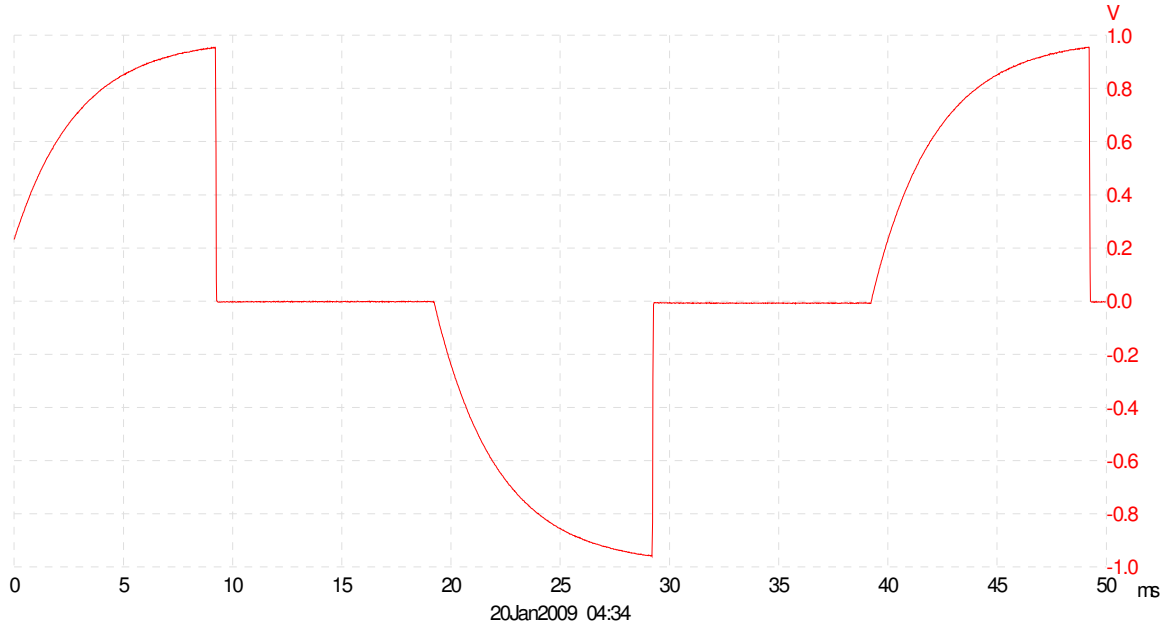


Figure B-1: High moment current waveform measured on 20th January 2009. Horizontal axis is time in ms. Vertical axis shows voltage measured using a current clamp (1 V = 100 A).

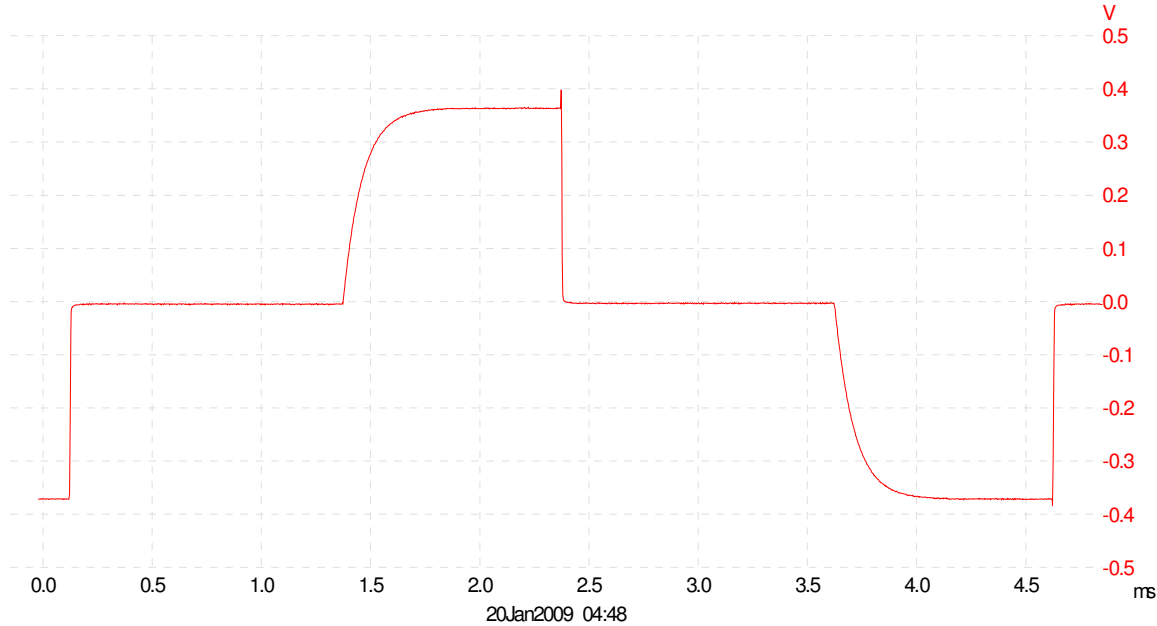


Figure B-2: Low moment current waveform measured on 20th January 2009. Horizontal axis is time in ms. Vertical axis shows voltage measured using a current clamp (1 V = 100 A).

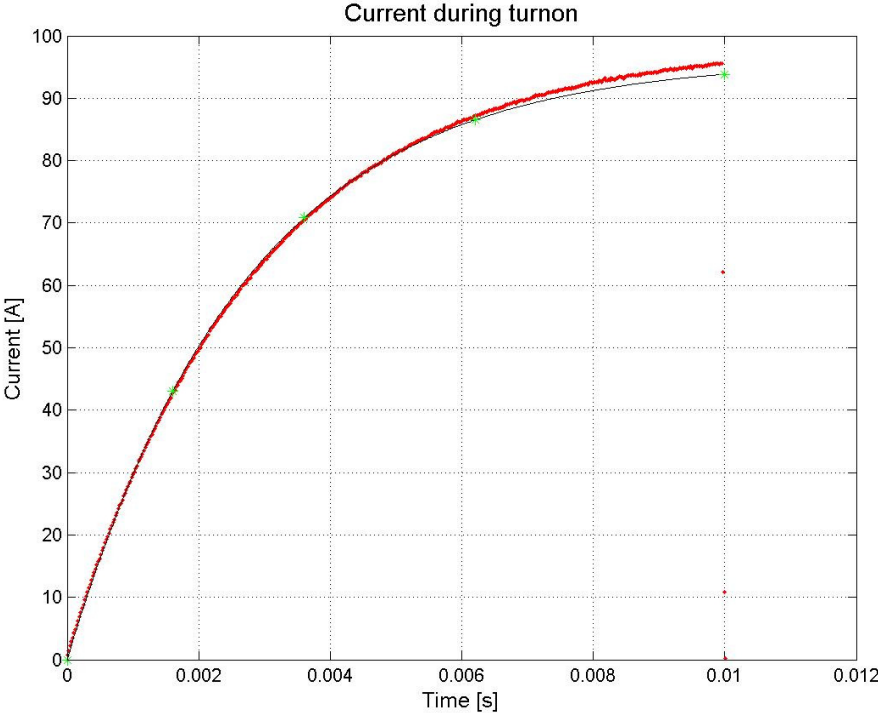


Figure B-3: High moment current turn-on measured on 20th January 2009.

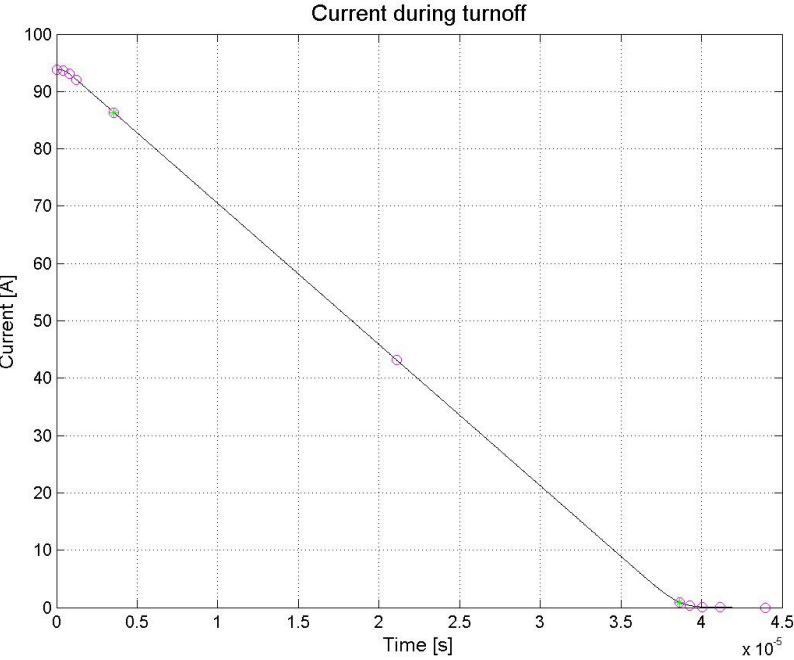


Figure B-4: High moment current turn-off measured on 20th January 2009.

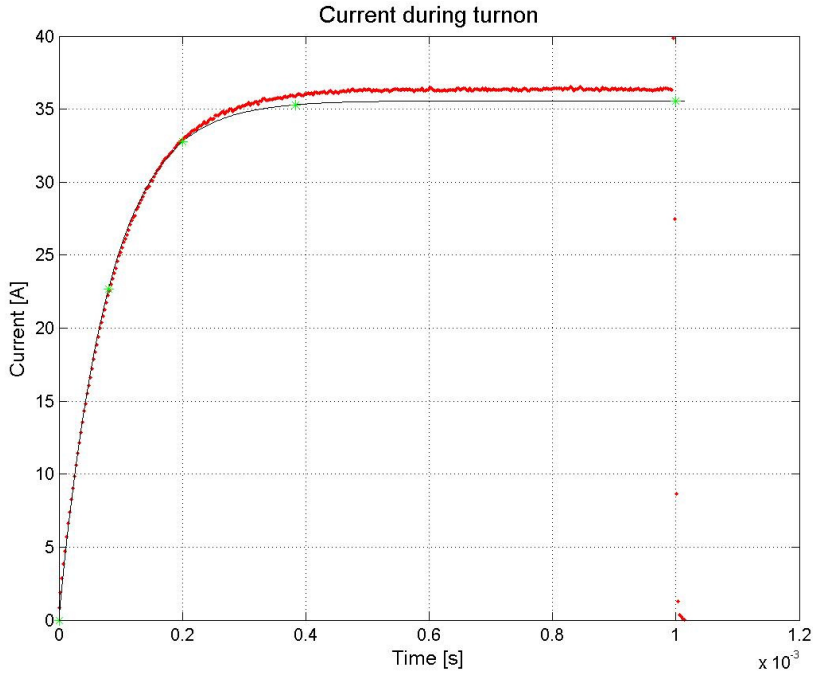


Figure B-5: Low moment current turn-on measured on 20th January 2009.

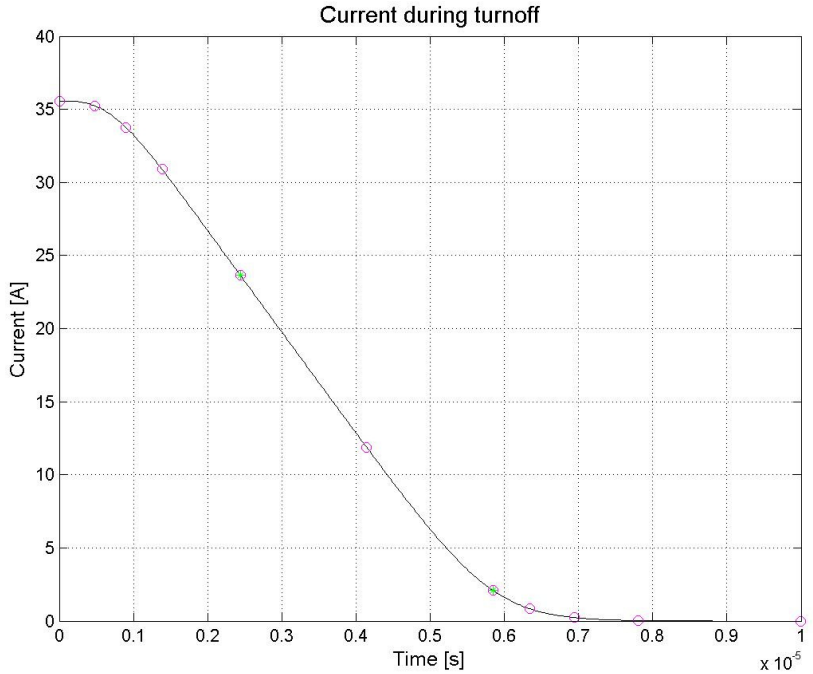


Figure B-6: Low moment current turn-off measured on 20th January 2009.

Appendix C High altitude tests

High altitude tests were conducted at the start and end of the survey.

Plots of the mean and standard deviation of the response at each channel are provided in Excel spreadsheets supplied with this report. All flights conducted met Geoforce quality control standards.

Plots of the mean channel amplitudes in the Excel spreadsheets show a nominal noise level for the high and low-moment data as an orange dashed line. This nominal noise corresponds to 10 nV/m^2 (voltage normalized by receiver area) at a delay time of 1 ms, which is a typical expected noise level for the SkyTEM system. When converted to survey EM units of $\text{V}/(\text{A.turns.m}^4)$ this noise level becomes $7.96\text{e-}13 \text{ V}/(\text{A.turns.m}^4)$ for low-moment data and $8.38\text{e-}14 \text{ V}/(\text{A.turns.m}^4)$ for high-moment data.

Note that laser altimeter data is null for all high altitude tests as the maximum range of the altimeters employed was 150 m. Magnetic (TMI) data has not been processed or supplied for the high altitude flights as these tests were performed for the purposes of EM quality control.

Appendix D Header for high moment SkyTEM data

| Column | Field | Format | Null value | Description | Units |
|-----------|-----------|--------|------------------|---|-----------------------------|
| Column 1 | Fid | I7 | 999999 | Geoforce Fiducial | n/a |
| Column 2 | Line | I8 | 99999 | Line Number | n/a |
| Column 3 | Flight | F11.1 | 99999999.9 | Flight number | n/a |
| Column 4 | DateTime | F17.10 | 99999.9999999999 | Decimal days since midnight, December 31st, 1899 | days |
| Column 5 | Date | I10 | 99999999 | Date (yyyymmdd) - GMT | n/a |
| Column 6 | Time | F12.3 | 999999.999 | Time (hhmmss.000) - GMT | n/a |
| Column 7 | AngleX | F8.3 | 999.999 | Tilt of frame from horizontal in flight direction | degrees |
| Column 8 | AngleY | F8.3 | 999.999 | Tilt of frame from horizontal perpendicular to flight direction | degrees |
| Column 9 | LasAlt | F8.1 | 99999.9 | Laser altitude of Tx loop centre (average of lasers 1 and 2) | metres |
| Column 10 | DTM_AHD | F8.1 | 99999.9 | Digital terrain model: corrected to AHD | metres |
| Column 11 | Current | F8.2 | 999.99 | Peak transmitter current | Amperes |
| Column 12 | North_AGD | F10.1 | 9999999.9 | Northing (AMG55/AGD66) | metres |
| Column 13 | East_AGD | F10.1 | 999999.9 | Easting (AMG55/AGD66) | metres |
| Column 14 | GpsAlt | F9.1 | 9999.9 | GPS Elevation of Tx loop centre: (GRS80) | metres |
| Column 15 | Gdspeed | F8.1 | 999.9 | Ground speed | km/hr |
| Column 16 | _2_Z2_1 | E13.5 | 1.00000E+33 | Normalised voltage Z-component Channel 1 | V/(A.turns.m ⁴) |
| Column 17 | _2_Z2_2 | E13.5 | 1.00000E+33 | Normalised voltage Z-component Channel 2 | V/(A.turns.m ⁴) |
| Column 18 | _2_Z2_3 | E13.5 | 1.00000E+33 | Normalised voltage Z-component Channel 3 | V/(A.turns.m ⁴) |
| Column 19 | _2_Z2_4 | E13.5 | 1.00000E+33 | Normalised voltage Z-component Channel 4 | V/(A.turns.m ⁴) |
| Column 20 | _2_Z2_5 | E13.5 | 1.00000E+33 | Normalised voltage Z-component Channel 5 | V/(A.turns.m ⁴) |
| Column 21 | _2_Z2_6 | E13.5 | 1.00000E+33 | Normalised voltage Z-component Channel 6 | V/(A.turns.m ⁴) |
| Column 22 | _2_Z2_7 | E13.5 | 1.00000E+33 | Normalised voltage Z-component Channel 7 | V/(A.turns.m ⁴) |
| Column 23 | _2_Z2_8 | E13.5 | 1.00000E+33 | Normalised voltage Z-component Channel 8 | V/(A.turns.m ⁴) |
| Column 24 | _2_Z2_9 | E13.5 | 1.00000E+33 | Normalised voltage Z-component Channel 9 | V/(A.turns.m ⁴) |
| Column 25 | _2_Z2_10 | E13.5 | 1.00000E+33 | Normalised voltage Z-component Channel 10 | V/(A.turns.m ⁴) |
| Column 26 | _2_Z2_11 | E13.5 | 1.00000E+33 | Normalised voltage Z-component Channel 11 | V/(A.turns.m ⁴) |

| | | | | | |
|------------------|----------------|-------|-------------|---|-----------------------------|
| Column 27 | <u>2_Z2_12</u> | E13.5 | 1.00000E+33 | Normalised voltage Z-component Channel 12 | V/(A.turns.m ⁴) |
| Column 28 | <u>2_Z2_13</u> | E13.5 | 1.00000E+33 | Normalised voltage Z-component Channel 13 | V/(A.turns.m ⁴) |
| Column 29 | <u>2_Z2_14</u> | E13.5 | 1.00000E+33 | Normalised voltage Z-component Channel 14 | V/(A.turns.m ⁴) |
| Column 30 | <u>2_Z2_15</u> | E13.5 | 1.00000E+33 | Normalised voltage Z-component Channel 15 | V/(A.turns.m ⁴) |
| Column 31 | <u>2_Z2_16</u> | E13.5 | 1.00000E+33 | Normalised voltage Z-component Channel 16 | V/(A.turns.m ⁴) |
| Column 32 | <u>2_Z2_17</u> | E13.5 | 1.00000E+33 | Normalised voltage Z-component Channel 17 | V/(A.turns.m ⁴) |
| Column 33 | <u>2_Z2_18</u> | E13.5 | 1.00000E+33 | Normalised voltage Z-component Channel 18 | V/(A.turns.m ⁴) |
| Column 34 | <u>2_Z2_19</u> | E13.5 | 1.00000E+33 | Normalised voltage Z-component Channel 19 | V/(A.turns.m ⁴) |
| Column 35 | <u>2_Z2_20</u> | E13.5 | 1.00000E+33 | Normalised voltage Z-component Channel 20 | V/(A.turns.m ⁴) |
| Column 36 | <u>2_Z2_21</u> | E13.5 | 1.00000E+33 | Normalised voltage Z-component Channel 21 | V/(A.turns.m ⁴) |
| Column 37 | <u>2_Z2_22</u> | E13.5 | 1.00000E+33 | Normalised voltage Z-component Channel 22 | V/(A.turns.m ⁴) |
| Column 38 | <u>2_Z2_23</u> | E13.5 | 1.00000E+33 | Normalised voltage Z-component Channel 23 | V/(A.turns.m ⁴) |
| Column 39 | <u>2_Z2_24</u> | E13.5 | 1.00000E+33 | Normalised voltage Z-component Channel 24 | V/(A.turns.m ⁴) |
| Column 40 | <u>2_Z2_25</u> | E13.5 | 1.00000E+33 | Normalised voltage Z-component Channel 25 | V/(A.turns.m ⁴) |
| Column 41 | <u>2_Z2_26</u> | E13.5 | 1.00000E+33 | Normalised voltage Z-component Channel 26 | V/(A.turns.m ⁴) |
| Column 42 | <u>2_Z2_27</u> | E13.5 | 1.00000E+33 | Normalised voltage Z-component Channel 27 | V/(A.turns.m ⁴) |
| Column 43 | <u>2_Z2_28</u> | E13.5 | 1.00000E+33 | Normalised voltage Z-component Channel 28 | V/(A.turns.m ⁴) |
| Column 44 | <u>2_Z2_29</u> | E13.5 | 1.00000E+33 | Normalised voltage Z-component Channel 29 | V/(A.turns.m ⁴) |
| Column 45 | <u>2_Z2_30</u> | E13.5 | 1.00000E+33 | Normalised voltage Z-component Channel 30 | V/(A.turns.m ⁴) |
| Column 46 | <u>2_Z2_31</u> | E13.5 | 1.00000E+33 | Normalised voltage Z-component Channel 31 | V/(A.turns.m ⁴) |
| Column 47 | <u>2_Z2_32</u> | E13.5 | 1.00000E+33 | Normalised voltage Z-component Channel 32 | V/(A.turns.m ⁴) |
| Column 48 | <u>4_X2_1</u> | E13.5 | 1.00000E+33 | Normalised voltage X-component Channel 1 | V/(A.turns.m ⁴) |
| Column 49 | <u>4_X2_2</u> | E13.5 | 1.00000E+33 | Normalised voltage X-component Channel 2 | V/(A.turns.m ⁴) |
| Column 50 | <u>4_X2_3</u> | E13.5 | 1.00000E+33 | Normalised voltage X-component Channel 3 | V/(A.turns.m ⁴) |
| Column 51 | <u>4_X2_4</u> | E13.5 | 1.00000E+33 | Normalised voltage X-component Channel 4 | V/(A.turns.m ⁴) |
| Column 52 | <u>4_X2_5</u> | E13.5 | 1.00000E+33 | Normalised voltage X-component Channel 5 | V/(A.turns.m ⁴) |
| Column 53 | <u>4_X2_6</u> | E13.5 | 1.00000E+33 | Normalised voltage X-component Channel 6 | V/(A.turns.m ⁴) |
| Column 54 | <u>4_X2_7</u> | E13.5 | 1.00000E+33 | Normalised voltage X-component Channel 7 | V/(A.turns.m ⁴) |
| Column 55 | <u>4_X2_8</u> | E13.5 | 1.00000E+33 | Normalised voltage X-component Channel 8 | V/(A.turns.m ⁴) |
| Column 56 | <u>4_X2_9</u> | E13.5 | 1.00000E+33 | Normalised voltage X-component Channel 9 | V/(A.turns.m ⁴) |

| | | | | | |
|------------------|----------|-------|-------------|---|-----------------------------|
| Column 57 | _4_X2_10 | E13.5 | 1.00000E+33 | Normalised voltage X-component Channel 10 | V/(A.turns.m ⁴) |
| Column 58 | _4_X2_11 | E13.5 | 1.00000E+33 | Normalised voltage X-component Channel 11 | V/(A.turns.m ⁴) |
| Column 59 | _4_X2_12 | E13.5 | 1.00000E+33 | Normalised voltage X-component Channel 12 | V/(A.turns.m ⁴) |
| Column 60 | _4_X2_13 | E13.5 | 1.00000E+33 | Normalised voltage X-component Channel 13 | V/(A.turns.m ⁴) |
| Column 61 | _4_X2_14 | E13.5 | 1.00000E+33 | Normalised voltage X-component Channel 14 | V/(A.turns.m ⁴) |
| Column 62 | _4_X2_15 | E13.5 | 1.00000E+33 | Normalised voltage X-component Channel 15 | V/(A.turns.m ⁴) |
| Column 63 | _4_X2_16 | E13.5 | 1.00000E+33 | Normalised voltage X-component Channel 16 | V/(A.turns.m ⁴) |
| Column 64 | _4_X2_17 | E13.5 | 1.00000E+33 | Normalised voltage X-component Channel 17 | V/(A.turns.m ⁴) |
| Column 65 | _4_X2_18 | E13.5 | 1.00000E+33 | Normalised voltage X-component Channel 18 | V/(A.turns.m ⁴) |
| Column 66 | _4_X2_19 | E13.5 | 1.00000E+33 | Normalised voltage X-component Channel 19 | V/(A.turns.m ⁴) |
| Column 67 | _4_X2_20 | E13.5 | 1.00000E+33 | Normalised voltage X-component Channel 20 | V/(A.turns.m ⁴) |
| Column 68 | _4_X2_21 | E13.5 | 1.00000E+33 | Normalised voltage X-component Channel 21 | V/(A.turns.m ⁴) |
| Column 69 | _4_X2_22 | E13.5 | 1.00000E+33 | Normalised voltage X-component Channel 22 | V/(A.turns.m ⁴) |
| Column 70 | _4_X2_23 | E13.5 | 1.00000E+33 | Normalised voltage X-component Channel 23 | V/(A.turns.m ⁴) |
| Column 71 | _4_X2_24 | E13.5 | 1.00000E+33 | Normalised voltage X-component Channel 24 | V/(A.turns.m ⁴) |
| Column 72 | _4_X2_25 | E13.5 | 1.00000E+33 | Normalised voltage X-component Channel 25 | V/(A.turns.m ⁴) |
| Column 73 | _4_X2_26 | E13.5 | 1.00000E+33 | Normalised voltage X-component Channel 26 | V/(A.turns.m ⁴) |
| Column 74 | _4_X2_27 | E13.5 | 1.00000E+33 | Normalised voltage X-component Channel 27 | V/(A.turns.m ⁴) |
| Column 75 | _4_X2_28 | E13.5 | 1.00000E+33 | Normalised voltage X-component Channel 28 | V/(A.turns.m ⁴) |
| Column 76 | _4_X2_29 | E13.5 | 1.00000E+33 | Normalised voltage X-component Channel 29 | V/(A.turns.m ⁴) |
| Column 77 | _4_X2_30 | E13.5 | 1.00000E+33 | Normalised voltage X-component Channel 30 | V/(A.turns.m ⁴) |
| Column 78 | _4_X2_31 | E13.5 | 1.00000E+33 | Normalised voltage X-component Channel 31 | V/(A.turns.m ⁴) |
| Column 79 | _4_X2_32 | E13.5 | 1.00000E+33 | Normalised voltage X-component Channel 32 | V/(A.turns.m ⁴) |
| Column 80 | N | F10.1 | 9999999.9 | Northing (MGA55/GDA94) | metres |
| Column 81 | E | F10.1 | 999999.9 | Easting (MGA55/GDA94) | metres |

Appendix E Header for low moment SkyTEM data

| Column | Field | Format | Null value | Description | Units |
|-----------|-----------|--------|------------------|---|-----------------------------|
| Column 1 | Fid | I7 | 999999 | Geoforce Fiducial | n/a |
| Column 2 | Line | I8 | 99999 | Line Number | n/a |
| Column 3 | Flight | F11.1 | 99999999.9 | Flight number | n/a |
| Column 4 | DateTime | F17.10 | 99999.9999999999 | Decimal days since midnight, December 31st, 1899 | days |
| Column 5 | Date | I10 | 99999999 | Date (yyyymmdd) - GMT | n/a |
| Column 6 | Time | F12.3 | 999999.999 | Time (hhmmss.000) - GMT | n/a |
| Column 7 | AngleX | F8.3 | 999.999 | Tilt of frame from horizontal in flight direction | degrees |
| Column 8 | AngleY | F8.3 | 999.999 | Tilt of frame from horizontal perpendicular to flight direction | degrees |
| Column 9 | LasAlt | F8.1 | 99999.9 | Laser altitude of Tx loop centre (average of lasers 1 and 2) | metres |
| Column 10 | DTM_AHD | F8.1 | 99999.9 | Digital terrain model: corrected to AHD | metres |
| Column 11 | Current | F8.2 | 999.99 | Peak transmitter current | Amperes |
| Column 12 | North_AGD | F10.1 | 9999999.9 | Northing (AMG55/AGD66) | metres |
| Column 13 | East_AGD | F10.1 | 9999999.9 | Easting (AMG55/AGD66) | metres |
| Column 14 | GpsAlt | F9.1 | 9999.9 | GPS Elevation of Tx loop centre: (GRS80) | metres |
| Column 15 | Gdspeed | F8.1 | 999.9 | Ground speed | km/hr |
| Column 16 | _1_Z2_1 | E13.5 | 1.00000E+33 | Normalised voltage Z-component Channel 1 | V/(A.turns.m ⁴) |
| Column 17 | _1_Z2_2 | E13.5 | 1.00000E+33 | Normalised voltage Z-component Channel 2 | V/(A.turns.m ⁴) |
| Column 18 | _1_Z2_3 | E13.5 | 1.00000E+33 | Normalised voltage Z-component Channel 3 | V/(A.turns.m ⁴) |
| Column 19 | _1_Z2_4 | E13.5 | 1.00000E+33 | Normalised voltage Z-component Channel 4 | V/(A.turns.m ⁴) |
| Column 20 | _1_Z2_5 | E13.5 | 1.00000E+33 | Normalised voltage Z-component Channel 5 | V/(A.turns.m ⁴) |
| Column 21 | _1_Z2_6 | E13.5 | 1.00000E+33 | Normalised voltage Z-component Channel 6 | V/(A.turns.m ⁴) |
| Column 22 | _1_Z2_7 | E13.5 | 1.00000E+33 | Normalised voltage Z-component Channel 7 | V/(A.turns.m ⁴) |
| Column 23 | _1_Z2_8 | E13.5 | 1.00000E+33 | Normalised voltage Z-component Channel 8 | V/(A.turns.m ⁴) |
| Column 24 | _1_Z2_9 | E13.5 | 1.00000E+33 | Normalised voltage Z-component Channel 9 | V/(A.turns.m ⁴) |
| Column 25 | _1_Z2_10 | E13.5 | 1.00000E+33 | Normalised voltage Z-component Channel 10 | V/(A.turns.m ⁴) |
| Column 26 | _1_Z2_11 | E13.5 | 1.00000E+33 | Normalised voltage Z-component Channel 11 | V/(A.turns.m ⁴) |
| Column 27 | _1_Z2_12 | E13.5 | 1.00000E+33 | Normalised voltage Z-component Channel 12 | V/(A.turns.m ⁴) |

| | | | | | |
|------------------|-----------------|-------|-------------|---|-----------------------------|
| Column 28 | <u>_1_Z2_13</u> | E13.5 | 1.00000E+33 | Normalised voltage Z-component Channel 13 | V/(A.turns.m ⁴) |
| Column 29 | <u>_1_Z2_14</u> | E13.5 | 1.00000E+33 | Normalised voltage Z-component Channel 14 | V/(A.turns.m ⁴) |
| Column 30 | <u>_1_Z2_15</u> | E13.5 | 1.00000E+33 | Normalised voltage Z-component Channel 15 | V/(A.turns.m ⁴) |
| Column 31 | <u>_1_Z2_16</u> | E13.5 | 1.00000E+33 | Normalised voltage Z-component Channel 16 | V/(A.turns.m ⁴) |
| Column 32 | <u>_1_Z2_17</u> | E13.5 | 1.00000E+33 | Normalised voltage Z-component Channel 17 | V/(A.turns.m ⁴) |
| Column 33 | <u>_1_Z2_18</u> | E13.5 | 1.00000E+33 | Normalised voltage Z-component Channel 18 | V/(A.turns.m ⁴) |
| Column 34 | <u>_1_Z2_19</u> | E13.5 | 1.00000E+33 | Normalised voltage Z-component Channel 19 | V/(A.turns.m ⁴) |
| Column 35 | <u>_1_Z2_20</u> | E13.5 | 1.00000E+33 | Normalised voltage Z-component Channel 20 | V/(A.turns.m ⁴) |
| Column 36 | <u>_1_Z2_21</u> | E13.5 | 1.00000E+33 | Normalised voltage Z-component Channel 21 | V/(A.turns.m ⁴) |
| Column 37 | <u>_1_Z2_22</u> | E13.5 | 1.00000E+33 | Normalised voltage Z-component Channel 22 | V/(A.turns.m ⁴) |
| Column 38 | <u>_3_X2_1</u> | E13.5 | 1.00000E+33 | Normalised voltage X-component Channel 1 | V/(A.turns.m ⁴) |
| Column 39 | <u>_3_X2_2</u> | E13.5 | 1.00000E+33 | Normalised voltage X-component Channel 2 | V/(A.turns.m ⁴) |
| Column 40 | <u>_3_X2_3</u> | E13.5 | 1.00000E+33 | Normalised voltage X-component Channel 3 | V/(A.turns.m ⁴) |
| Column 41 | <u>_3_X2_4</u> | E13.5 | 1.00000E+33 | Normalised voltage X-component Channel 4 | V/(A.turns.m ⁴) |
| Column 42 | <u>_3_X2_5</u> | E13.5 | 1.00000E+33 | Normalised voltage X-component Channel 5 | V/(A.turns.m ⁴) |
| Column 43 | <u>_3_X2_6</u> | E13.5 | 1.00000E+33 | Normalised voltage X-component Channel 6 | V/(A.turns.m ⁴) |
| Column 44 | <u>_3_X2_7</u> | E13.5 | 1.00000E+33 | Normalised voltage X-component Channel 7 | V/(A.turns.m ⁴) |
| Column 45 | <u>_3_X2_8</u> | E13.5 | 1.00000E+33 | Normalised voltage X-component Channel 8 | V/(A.turns.m ⁴) |
| Column 46 | <u>_3_X2_9</u> | E13.5 | 1.00000E+33 | Normalised voltage X-component Channel 9 | V/(A.turns.m ⁴) |
| Column 47 | <u>_3_X2_10</u> | E13.5 | 1.00000E+33 | Normalised voltage X-component Channel 10 | V/(A.turns.m ⁴) |
| Column 48 | <u>_3_X2_11</u> | E13.5 | 1.00000E+33 | Normalised voltage X-component Channel 11 | V/(A.turns.m ⁴) |
| Column 49 | <u>_3_X2_12</u> | E13.5 | 1.00000E+33 | Normalised voltage X-component Channel 12 | V/(A.turns.m ⁴) |
| Column 50 | <u>_3_X2_13</u> | E13.5 | 1.00000E+33 | Normalised voltage X-component Channel 13 | V/(A.turns.m ⁴) |
| Column 51 | <u>_3_X2_14</u> | E13.5 | 1.00000E+33 | Normalised voltage X-component Channel 14 | V/(A.turns.m ⁴) |
| Column 52 | <u>_3_X2_15</u> | E13.5 | 1.00000E+33 | Normalised voltage X-component Channel 15 | V/(A.turns.m ⁴) |
| Column 53 | <u>_3_X2_16</u> | E13.5 | 1.00000E+33 | Normalised voltage X-component Channel 16 | V/(A.turns.m ⁴) |
| Column 54 | <u>_3_X2_17</u> | E13.5 | 1.00000E+33 | Normalised voltage X-component Channel 17 | V/(A.turns.m ⁴) |
| Column 55 | <u>_3_X2_18</u> | E13.5 | 1.00000E+33 | Normalised voltage X-component Channel 18 | V/(A.turns.m ⁴) |
| Column 56 | <u>_3_X2_19</u> | E13.5 | 1.00000E+33 | Normalised voltage X-component Channel 19 | V/(A.turns.m ⁴) |
| Column 57 | <u>_3_X2_20</u> | E13.5 | 1.00000E+33 | Normalised voltage X-component Channel 20 | V/(A.turns.m ⁴) |

| | | | | | |
|------------------|-----------------|-------|-------------|---|-----------------------------|
| Column 58 | <u>_3_X2_21</u> | E13.5 | 1.00000E+33 | Normalised voltage X-component Channel 21 | V/(A.turns.m ⁴) |
| Column 59 | <u>_3_X2_22</u> | E13.5 | 1.00000E+33 | Normalised voltage X-component Channel 22 | V/(A.turns.m ⁴) |
| Column 60 | N | F10.1 | 9999999.9 | Northing (MGA55/GDA94) | metres |
| Column 61 | E | F10.1 | 999999.9 | Easting (MGA55/GDA94) | metres |

Appendix F Header for TMI data

| Column | Field | Format | Null value | Description | Units | Sign convention |
|-----------|-------------|--------|-------------|--|--------|---------------------|
| Column 1 | Fid | I7 | 999999 | Geoforce Fiducial | n/a | |
| Column 2 | Line | I8 | 99999 | Line Number | n/a | |
| Column 3 | Flight | F11.1 | 99999999.9 | Flight number | n/a | |
| Column 4 | DateTime | F17.10 | 99999.99999 | Decimal days since midnight, December 31st, 1899 | days | Greenwich mean time |
| Column 5 | Date | I10 | 99999999 | Date (yyyymmdd) - GMT | n/a | Greenwich mean time |
| Column 6 | Time | F12.3 | 999999.999 | Time (hhmmss.000) - GMT | n/a | Greenwich mean time |
| Column 7 | NORTH_AGD | F10.1 | 9999999.9 | Northing (AGD66/AMG55) | metres | |
| Column 8 | EAST_AGD | F10.1 | 999999.9 | Easting (AGD66/AMG55) | metres | |
| Column 9 | GPSALT | F9.1 | 999.9 | GPS Elevation of Tx loop centre: (GRS80 Ellipsoid) | metres | |
| Column 10 | GDSPEED | F8.1 | 999.9 | Ground speed | km/hr | |
| Column 11 | MAG_RAW | F9.2 | 999999.9 | Raw total magnetic field strength | nT | |
| Column 12 | MAG_BASE | F9.2 | 999999.99 | Diurnal magnetic field strength | nT | |
| Column 13 | MAG_DIURNAL | F9.2 | 999999.99 | Diurnal corrected magnetic field | nT | |
| Column 14 | MAG_DI_IGRF | F9.2 | 999999.99 | IGRF and Diurnal corrected magnetic field | nT | |
| Column 15 | IGRF | F9.2 | 999999.99 | IGRF field strength | nT | |
| Column 16 | MAG_TLEV | F9.2 | 999999.99 | Tie line levelled magnetic field strength | nT | |
| Column 17 | MAG_MLEV | F9.2 | 999999.99 | Micro levelled magnetic field strength | nT | |
| Column 18 | TMI | F9.2 | 999999.99 | TMI (MAG_MLEV + IGRF) | nT | |

| | | | | | |
|----------------------|---|-------|-----------|------------------------|--------|
| Column 19 | N | F10.1 | 9999999.9 | Northing (GDA94/MGA55) | metres |
| Column 20 | E | F10.1 | 9999999.9 | Easting (GDA94/MGA55) | metres |

Appendix G Header for CDI data

| Column | Field | Start column | End column | Format | Null value | Description | Units | Sign convention |
|-----------|----------|--------------|------------|--------|------------|--|--------|-------------------|
| Column 1 | Line | 4 | 10 | I7 | 9999999 | Line Number | n/a | |
| Column 2 | Easting | 12 | 20 | F9.2 | 999999.99 | Easting (AGD66/AMG55) | metres | |
| Column 3 | Northing | 22 | 31 | F10.2 | 9999999.99 | Northing (AGD66/AMG55) | metres | |
| Column 4 | Dist | 34 | 41 | F8.2 | 99999.99 | Distance along line | metres | |
| Column 5 | Depth | 45 | 51 | F7.2 | 9999.99 | Depth | n/a | -ve below surface |
| Column 6 | Cond | 54 | 62 | F9.4 | 9999.9999 | Conductivity | mS/m | |
| Column 7 | Elev | 66 | 72 | F7.2 | 9999.99 | Elevation corresponding to depth in Column 5 | metres | |
| Column 8 | Time | 76 | 82 | F7.2 | 9999.99 | Delay time | µs | Start of ramp |
| Column 9 | Alt | 87 | 92 | F6.2 | 999.99 | Laser Altimeter | metres | |
| Column 10 | TxElev | 96 | 102 | F7.2 | 9999.99 | GPS Elevation of Tx loop centre: (GRS80 Ellipsoid) | metres | |
| Column 11 | DEM | 106 | 112 | F7.2 | 9999.99 | Digital elevation model (AHD) | metres | |

| Appendix H | | Header for conductivity-depth slice data | | | | | |
|-------------------|--------------|---|-------------------|---------------|-------------------|--|--------------|
| Column | Field | Start column | End column | Format | Null value | Description | Units |
| Column 1 | Line | 3 | 9 | I7 | 9999999 | Line Number | n/a |
| Column 2 | Easting | 12 | 19 | F8.1 | 999999.9 | Easting (AGD66/AMG55) | metres |
| Column 3 | Northing | 23 | 31 | F9.1 | 9999999.9 | Northing (AGD66/AMG55) | metres |
| Column 4 | Av0_5 | 34 | 45 | E12.6 | 0.999990e+05 | Average conductivity in depth slice 0 to 5 m below surface | mS/m |
| Column 5 | Av5_10 | 48 | 59 | E12.6 | 0.999990e+05 | Average conductivity in depth slice 5 to 10 m below surface | mS/m |
| Column 6 | Av10_15 | 62 | 73 | E12.6 | 0.999990e+05 | Average conductivity in depth slice 10 to 15 m below surface | mS/m |
| Column 7 | Av15_20 | 76 | 87 | E12.6 | 0.999990e+05 | Average conductivity in depth slice 15 to 20 m below surface | mS/m |
| Column 8 | Av20_30 | 90 | 101 | E12.6 | 0.999990e+05 | Average conductivity in depth slice 20 to 30 m below surface | mS/m |
| Column 9 | Av30_40 | 104 | 115 | E12.6 | 0.999990e+05 | Average conductivity in depth slice 30 to 40 m below surface | mS/m |
| Column 10 | Av40_60 | 118 | 129 | E12.6 | 0.999990e+05 | Average conductivity in depth slice 40 to 60 m below surface | mS/m |
| Column 11 | Av60_100 | 132 | 143 | E12.6 | 0.999990e+05 | Average conductivity in depth slice 60 to 100 m below surface | mS/m |
| Column 12 | Av100_150 | 146 | 157 | E12.6 | 0.999990e+05 | Average conductivity in depth slice 100 to 150 m below surface | mS/m |

| | | | | | | | |
|------------------|-----------|-----|-----|-------|--------------|--|------|
| Column 13 | Av150_200 | 160 | 171 | E12.6 | 0.999990e+05 | Average conductivity in depth slice 150 to 200 m below surface | mS/m |
| Column 14 | Av200plus | 174 | 185 | E12.6 | 0.999990e+05 | Average conductivity in depth slice > 200m below surface | mS/m |

Appendix I Deliverables on DVD

The following folders of data are included with this report on DVD. Each directory has a text file description explaining the data format of the raw files inside.

| Folder | Description | File Type |
|------------------|--|------------------|
| AEM_Binary | Raw (binary) data from SkyTEM EM system | ASCII & Binary |
| AEM_Grids | Grids of EM data | .ers |
| AEM_Images | Images of EM grids | .jpg |
| AEM_Located | Header explanation and ASCII data file for processed EM data | ASCII & .pdf |
| AHD Value | Text file of 'N' value added to bring DEM data up to AHD values | ASCII |
| ASEG_GDF | Header, data and description files in ASEG GDF format | ASCII |
| CDI_Depth_Slices | ASCII data file of average conductivity within specified depth intervals below surface | ASCII |
| CDI_Images | Section Images of CDI data | .jpg |
| CDI_Located | Header explanation and ASCII data file for processed CDI data | ASCII & .pdf |
| CurrentWaveform | Transmitter loop current waveform check raw data and images | ASCII & .jpg |
| High_Alt_Tests | Excel spreadsheets of high altitude EM data | .xlsx |
| Line Statistics | Clearance and speed statistics | .xlsx |
| Linefile | Line start and end co ordinates and times | ASCII |
| Logistics Report | Summary of field crew activity for survey | .pdf |
| Mag_Base | Base Magnetometer location | ASCII |
| Mag_Binary | Raw (binary) data from SkyTEM magnetics system | ASCII & Binary |
| Mag_Located | Header explanation and ASCII data file for processed magnetic data | ASCII & .pdf |